

PHYSICAL REVIEW B

CONDENSED MATTER

THIRD SERIES, VOLUME 45, NUMBER 16

15 APRIL 1992-II

Reexamination of the electron band structure of Tb along the $\Gamma\Delta A$ line

S. C. Wu,* H. Li,[†] Y. S. Li, D. Tian, J. Quinn, and F. Jona

College of Engineering and Applied Science, State University of New York, Stony Brook, New York 11794

D. Fort

School of Metallurgy and Materials, University of Birmingham, Birmingham B15 2TT, England

N. E. Christensen

Institute of Physics, Aarhus University, DK-8000 Aarhus C, Denmark

(Received 27 June 1991)

The electron band structure of Tb metal has been reexamined by means of angle-resolved photoemission experiments on Tb(0001) samples free of Fe impurities in the surface region. Comparison of the present data with those collected from an Fe-contaminated sample shows that the presence of Fe in the surface region caused a shift of the top portion of the $6s-5d_{3z^2-1}$ -type Δ_1 band toward larger binding energies by approximately 1 eV. The energy position of the top of the Δ_1 band (Γ_4^-) is -2.6 eV. The agreement with the result of the relativistic linear-muffin-tin-orbital calculation reported earlier ($E_{\Gamma_4^-} = -2.3$ eV) is markedly improved.

I. INTRODUCTION

The study of the physical and chemical properties of rare-earth metals presents a strong challenge to the experimentalist owing to the pronounced chemical reactivity of these metals, which makes it very difficult to grow pure single crystals and to prepare and maintain atomically clean surfaces.¹ We recently reported² an investigation of the electron band structure of Tb by means of angle-resolved photoemission experiments, but the sample used in that investigation was found to contain Fe impurities that segregated on the surface in substantial amounts. The impurities apparently only affected the density of states near the Fermi level and did not prevent the observation of a dispersing band, which was identified as the $6s-5d_{3z^2-1}$ -type Δ_1 band—hence, it was believed that the presence of Fe would have no effect on the band-mapping process.

Subsequently, a purer sample of Tb, prepared in the School of Metallurgy and Materials of the University of Birmingham (UK), became available and this sample made it possible to develop and test cleaning procedures for the elimination of impurities from the surface region and hence to study the properties of a clean surface. Thus, a quantitative low-energy-electron-diffraction (LEED) study of a clean Tb(0001) surface was carried out,³ which found a first-interlayer contraction of 3.9%

and a second-interlayer expansion of 1.4% with respect to the bulk spacing. In addition, a photoemission study revealed the presence of a surface state on clean Tb(0001) which lies 0.5 eV below the Fermi level and inside an energy gap of the projected band structure at the center of the Brillouin zone, $\bar{\Gamma}$.⁴

In the present paper we report angle-resolved photoemission data from clean Tb(0001) which demonstrate that the presence of large amounts of Fe in the surface region of the earlier sample had caused the $6s-5d_{3z^2-1}$ -type Δ_1 band to shift toward larger binding energies by about 1 eV. This shift can be explained by the repulsion between the Fe $3d$ and the Tb $5d$ electrons. The present data in fact produce much better agreement between experimental and theoretical bands.²

We give below some experimental details in Sec. II, present the results in Sec. III, and draw the conclusions in Sec. IV.

II. EXPERIMENTAL PROCEDURES

The photoemission experiments were carried out at beamline U7B of the National Synchrotron Light Source at the Brookhaven National Laboratory. A plane-grating monochromator was used to disperse the synchrotron light. The photoelectron energies were measured with an angle-resolved double-pass cylindrical mirror analyzer

(CMA) fitted with a special slit providing an angular resolution of 4° . Less resolution than in the previous study of Tb(0001) (2° in Ref. 2) was chosen in order to gain intensity and therefore shorten data-collection time. The same CMA was also used to monitor the chemical condition of the surface by Auger-electron spectroscopy (AES), while LEED was used to monitor the crystallinity of the surface.

The experiments were done on two Tb samples, both present in the experimental chamber in the same run. Both samples were mounted on a manipulator that allowed either one to be moved in the proper position for LEED or photoemission experiments.⁵ This manipulator also allowed rotations around three mutually perpendicular axes, so that photoemission experiments could be done with either *s*- or *s-p*-polarized radiation up to 25% *p* polarization.

The two samples had different origins. Sample *A* was purchased from the Materials Preparation Center of the University of Iowa in Ames, Iowa, was cut from the same ingot, and was prepared in the same manner as the sample that we studied earlier.² In particular, the sample was electropolished in a bath that passivated the surface with a Cl layer. It was therefore expected that sample *A* would contain at least Cl and Fe impurities, according to our previous experience.² Sample *B* stemmed from a single crystal that was grown and purified by the electromigration process in the School of Metallurgy and Materials of the University of Birmingham (UK). This sample was mechanically polished as described elsewhere³ and was expected to contain less Fe impurity than sample *A*.

The elaborate procedures followed for the preparation of a clean surface have been described elsewhere⁴ and will not be discussed here. We will mention only that substantial segregation of Fe on the surface of sample *A* was found after high-temperature (650–800°C) anneals, in agreement with our earlier experience.² Figure 1 shows a typical AES scan from a surface that had been subjected to many hours of Ar-ion bombardments at about 750°C

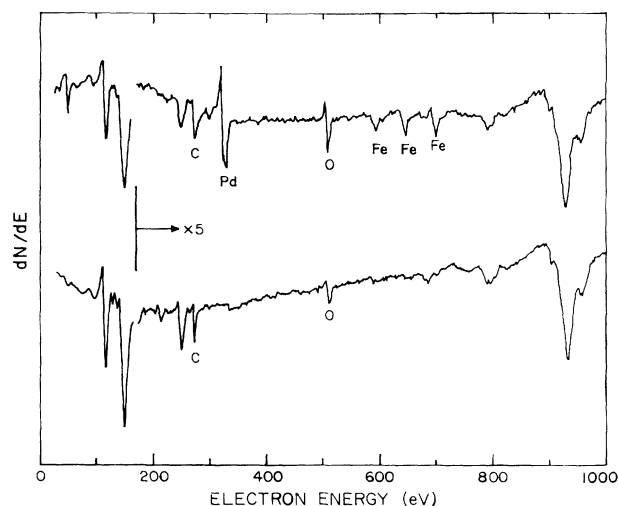


FIG. 1. AES scans from Tb(0001). Above: after 60 h of Ar-ion bombardments at about 750°C. Below: after prolonged Ar-ion bombardments at about 450°C (see Ref. 4).

(Pd and Fe lines are visible); and below, an AES scan from a surface depleted of metallic impurities but still contaminated with some C and O. These latter impurities originated from the residual atmosphere in the experimental chamber; they were not present on the surface immediately after the cleaning process, but increased in concentration with time and were notably enhanced by the impact of high-energy electrons such as are needed in AES experiments. Thus, to minimize the concentrations of C and O the surface was periodically recleaned approximately every 40 min and the photoemission data were collected immediately after the cleaning process and before the recording of AES scans. When clean, sample *A* gave the same results as sample *B*, thus providing confidence that these results reflect the properties of clean Tb(0001). For brevity, we show here only the results obtained with sample *B*.

III. RESULTS AND DISCUSSION

Figure 2 shows angle-resolved normal-emission spectra from clean Tb(0001) taken with 25% *p*-polarized radiation and photon energies between 14 and 38 eV. We note the presence of seven features, denoted by *A*, *B*, *C*, *D*, P_1 , P_2 , and *S* in the figure, which we discuss in the following.

Peaks *A* and *D*, located 2.6 and 7.7 eV below the Fermi level, respectively, are due to the *4f* electrons of Tb. Their energy positions are very close to those reported by Gerken *et al.*⁶ These peaks can be seen only with photon energies larger than 30 eV, because below 30 eV the photoionization cross section of the *4f* electrons is very low.⁷

Peak *S*, located about 0.5 eV below the Fermi level, is due to a surface state, as discussed elsewhere,⁴ and will not be discussed further here.

Peak *C*, located about 6 eV below the Fermi level, grew rather rapidly with time and is associated with oxygen contamination, as demonstrated by AES. Even at pressures of $(1-2) \times 10^{-10}$ Torr, the oxygen peak *C* became detectable already about 15 min after an ion-bombardment and annealing cycle. The electron-distribution curves (EDC's) shown in Fig. 2 were all collected within less than 40 min after each cleaning cycle. It may be useful, in this respect, to point out again (see Ref. 4) that the oxygen contamination was substantially reduced if, after cleaning, the surface was *not* exposed either to high-energy electrons (such as used for AES) or to high-intensity photons (such as needed for "zeroth-order alignment" of the monochromator).

Peak *B*, weak and identifiable only at low photon energies, disperses from -6.9 eV for photon energy $h\nu = 14$ eV to -2.6 eV for $h\nu = 18.5$ eV, and is due to direct transitions from the $6s-5d_{3z^2-1}$ -type Δ_1 band. (Study of the polarization dependence of this peak shows that it is *p* polarization sensitive, hence we deduce from the dipole selection rules that it is a Δ_1 band.) The fact that peak *B* does not disperse for $h\nu > 20$ eV is related to the short mean free path of the photoelectrons and the attendant strong k_{\perp} broadening, which increases the contribution of indirect transitions at the cost of direct transitions. Hence, in the photon-energy range above 20 eV peak *B* is dominated by transitions from regions of the band struc-

ture with high density of initial states (the top of the Δ_1 band, Γ_4^-).

Peaks P_1 and P_2 stem from the Tb $5p_{3/2}$ level and are due to electrons emitted by second-order light produced by the monochromator, i.e., by photons with energy $2h\nu$. We prove this statement in the following.

In the photon-energy range between 18 and 21 eV peaks P_1 and P_2 shift to smaller binding energy with increasing photon energy (see Fig. 2). Figure 3(a) depicts an EDC of the Tb $4p$ levels with $h\nu=40$ eV. We see three features, P_1 , P_2 , and P_3 , located 21.2, 22.6, and 28.7 eV below the Fermi level, respectively. Feature P_3

originates from the $5p_{1/2}$ level, while P_1 and P_2 originate from the $5p_{3/2}$ level. The binding energies of P_2 (the larger feature in the broad $5p_{3/2}$ spectrum) and P_3 are consistent with the values published in the table of electron binding energies edited by Cardona and Ley.⁸

First, we note that the kinetic energy of the electrons emitted by the second-order light from the $5p_{3/2}$ level is $E_K=2h\nu-E_b$, where E_b is the binding energy of the $5p_{3/2}$ level [21.2 and 22.6 eV for P_1 and P_2 , respectively, in Fig. 3(a)]. Hence, the "apparent" binding energy of these same electrons in the EDC's measured with photon energy $h\nu$ (Fig. 2) is given by $h\nu-E_K=E_b-h\nu$, as can be tested in Fig. 2.

Second, we note that the ratio of intensities of P_1 to P_2 is the same in Fig. 2 for $h\nu > 19$ eV as in Fig. 3. Third, we note that the EDC for $h\nu=21$ eV in Fig. 2 shows rather high counts in the energy range above the Fermi level. These three observations are consistent with the origin of peaks P_1 and P_2 from interference by second-order light.

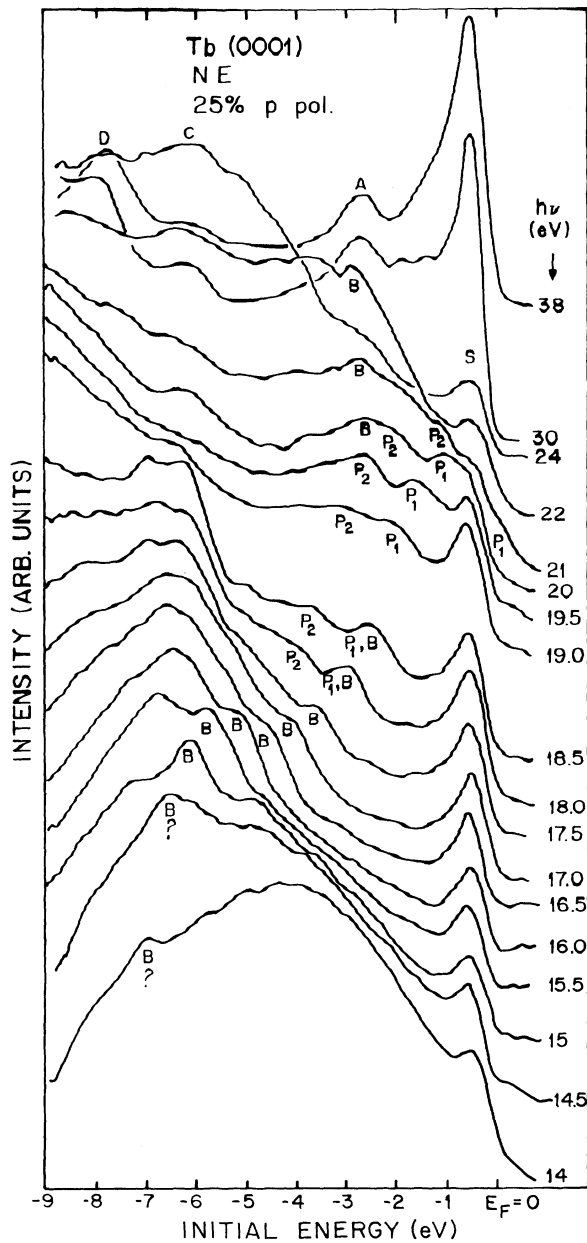


FIG. 2. Angle-resolved normal-emission electron distribution curves from Tb(0001) for 25% p -polarized photons between 14 and 38 eV. Peaks A , B , C , D , P_1 , P_2 , and S are discussed in the text.

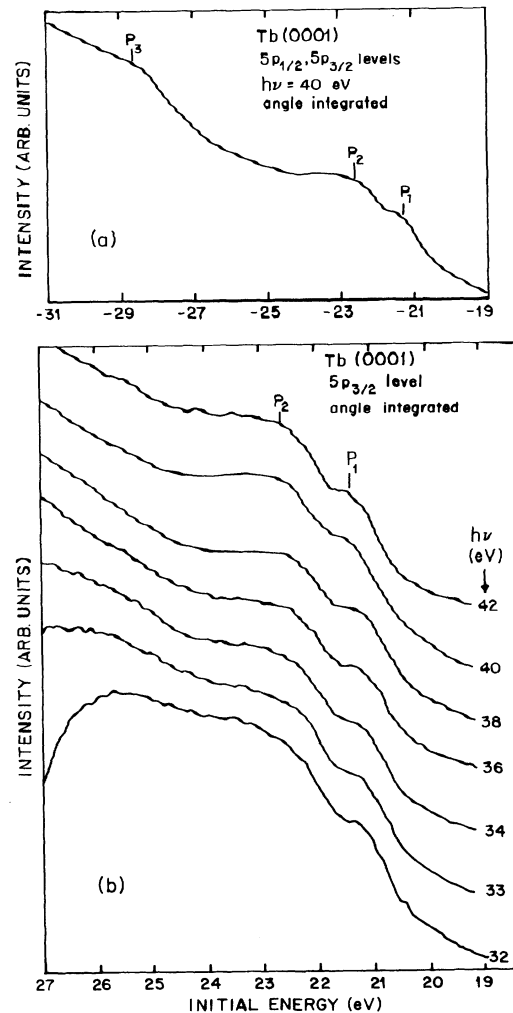


FIG. 3. (a) Angle-integrated photoemission from the Tb $5p_{1/2}$ and $5p_{3/2}$ levels with photon energy $h\nu=40$ eV. (b) Photon-energy dependence of photoemission from the Tb $5p_{3/2}$ level.

We also note that peaks P_1 and B overlap one another in the photon-energy range around 18 eV. In fact, we see in Fig. 3(b) that the intensity ratio of P_1 to P_2 is constant when the photon energy varies between 32 and 42 eV (corresponding to 16–21 eV in Fig. 2). But for $h\nu=18$ and 18.5 eV the intensity ratio P_1/P_2 is larger in Fig. 2 than in Fig. 3(b), demonstrating that peak P_1 has some contribution from peak B . For photon energies smaller than 17.5 eV peaks P_1 and P_2 are very weak and hence the effect of second-order light can be neglected.

Finally, we note that the photoionization cross section of Tb $5p$ electrons is high at photon energies around 40 eV (Ref. 7), and also that there is only one $5d$ electron in Tb, but there are four $5p$ electrons in the $5p_{3/2}$ level, all of which makes it understandable that the second-order light effect could be observed. On an Fe-contaminated surface² this effect was *not* observed, probably because it was obscured by the presence of Fe and by the short mean free path of electrons in Tb.

A careful comparison of the positions of peak B in Fig. 2 with those found on the Fe-contaminated surface in the earlier work² is instructive. We find that at photon energies smaller than 17 eV the peak positions are not very different in the two cases, but for photon energies between 17 and 18.5 eV peak B is consistently found at smaller binding energies by 0.5–1 eV. We conclude therefore that the presence of Fe in the earlier sample pushed at least the top portion of the Tb $6s-5d_{3z^2-1}$ -type Δ_1 band toward larger binding energies. This effect can be explained by the repulsion between the Fe $3d$ and the Tb $5d$ electrons. This repulsion is proportional to⁹

$$\langle \Psi_{\text{Fe}(3d)} | \Delta H | \Psi_{\text{Tb}(5d)} \rangle^2 / (E_{b[\text{Fe}(3d)]} - E_{b[\text{Tb}(5d)]}),$$

where $\Psi_{\text{Fe}(3d)}$ and $\Psi_{\text{Tb}(5d)}$ are the wave functions of the Fe $3d$ and Tb $5d$ electrons, respectively, ΔH is the Hamiltonian of the interaction between these two, and $E_{b[\text{Fe}(3d)]}$ and $E_{b[\text{Tb}(5d)]}$ are the binding energies of the Fe $3d$ and Tb $5d$ electrons, respectively. Since the center of the Fe $3d$ valence band is located about 0.5 eV below the Fermi level, the difference $E_{b[\text{Fe}(3d)]} - E_{b[\text{Tb}(5d)]}$ is smaller for electrons in the top portion of the Tb $5d$ valence band than for electrons in the bottom portion of that band, hence the repulsion is stronger for the former than for the latter. A similar repulsion effect has been observed in Cu_3Au between the Cu $3d$ and the Au $5d$ electrons.^{10,11} Also, LaGraffe, Dowben, and Onellion¹² reported energy shifts as large as 0.7 eV of the Cu $3d$ valence band at the interface between a copper substrate and a gadolinium film, and attributed this shift to the strong interaction between Cu and Gd. We note that the Tb $4f$ levels were not affected by the presence of Fe in our previous study²—a conclusion drawn from the comparison between the present data (without Fe) and the earlier data (with Fe). This observation can be explained by the fact that the Tb $4f$ electrons are very localized,¹³ and hence, the overlap between the wave functions of the Fe $3d$ and the Tb $4f$ electrons is much less than the overlap between the wave functions of the Fe $3d$ and the Tb $5d$ electrons.

We now discuss the problems encountered in the process of using the present data for the determination of the

band structure of Tb. Owing to the overlap between the top portion of the $6s-5d_{3z^2-1}$ -type Δ_1 band on one hand and the Tb $5p_{3/2}$ peak produced by the second-order light on the other, we found it difficult to determine the position of the top of the Δ_1 band from the EDC's in Fig. 2. In our earlier study² the position of the top of the Δ_1 band was confirmed by a resonance photoemission study, namely, on the Fe-contaminated Tb(0001) surface we had found that near the Tb $4d$ absorption edges (143–145 eV and 150–153 eV) the peak located at -3.6 eV (Γ_4^- , top of the Δ_1 band) exhibited different resonance behavior from the peak located at -2.6 eV (Tb $4f$ level). However, as Fig. 4 shows, on the present clean Tb(0001) surface we find only one peak, located at -2.6 eV, and this peak exhibits resonance behavior at photon energies near the Tb $4d$ absorption edge. This observation suggests that the top of the Δ_1 band (Γ_4^-) has the same binding energy as the Tb $4f$ band.

The mapping of the initial band from the present ex-

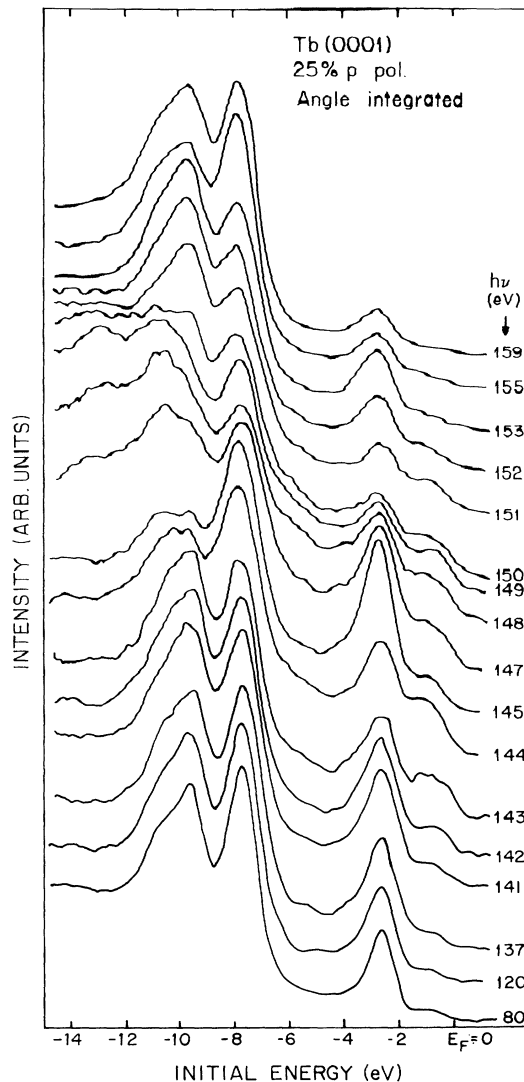


FIG. 4. Angle-integrated photoemission curves from clean Tb(0001) for photon energies between 80 and 159 eV.

perimental photoemission data was carried out with the same method used in the earlier study², i.e., the final band was obtained from a band in the effective-mass approximation as fitted to experimentally determined critical points. A difficulty is encountered, however, in trying to identify the position of the bottom of the band.

At low photon energies ($h\nu < 15$ eV), peak *B* is located in the high background produced by secondary electrons (see Fig. 2). We see that for $h\nu = 14.5$ eV the width of peak *B* is visibly larger than for larger photon energies, and we cannot exclude the possibility that below 15 eV peak *B* (shown with question marks in Fig. 2) is not due to a direct transition. Hence, we cannot decide with confidence whether the bottom of the band is located at -6.9 eV (EDC for $h\nu = 14$ eV in Fig. 2) or at -6.1 eV (EDC for $h\nu = 15$ eV in Fig. 2). The fact that peak *B* was never observed to return to smaller binding energies for $h\nu < 15$ eV is not useful to decide between the two alternatives because we know from theory² that there is an energy gap below Γ_4^- (10 eV above the Fermi level) along the $\Gamma\Delta A$ line, hence for photon energies below the value at which the final state reaches the Γ_4^- point peak *B* should disappear. We therefore leave both possibilities open for the position of the bottom of the band in the following evaluation of the $6s-5d_{3z^2-1}$ -type Δ_1 band.

If the bottom of the band is at -6.9 eV ($h\nu = 14$ eV), then the final-state energy $E_{\text{final}} = 7.1$ eV. If the bottom of the band is at -6.1 eV ($h\nu = 15$ eV), then $E_{\text{final}} = 8.9$ eV. In either case these values correspond to the Γ point $k_{\perp} = 2k_{\Gamma A}$ and in either case the final-state energy for $k_{\perp} = 4k_{\Gamma A}$ is 15.9 eV ($h\nu = 18.5$ eV). These final-energy values were used to fit the final-state band in the range $2k_{\Gamma A} \leq k_{\perp} \leq 4k_{\Gamma A}$ to the parabolic form

$$E_{\text{final}} - E_F = \frac{\hbar^2}{2m_e^*} k_{\text{final}}^2, \quad (1)$$

where E_F is the position of the bottom of the band relative to the Fermi level defined as the zero of energy, m_e^* is the effective mass, and k_{final} is the magnitude of the final-state wave vector. Thus, we find that the effective mass m_e^* is about $1.59m_e$ or $2.0m_e$ ($m_e = \text{free-electron mass}$), and $E_F = +4.2$ eV or $+6.6$ eV, respectively, for the two choices of the bottom of the band. (Note that the bottom of the band is higher than the Fermi level, owing to the presence of the $4f$ levels.) The final bands are different in the two cases and are shown as solid or dashed-dotted lines in the top portion of Fig. 5.

Accordingly, the experimental band structure is shown with full circles (solid line) or with crosses (dashed-dotted line) in the bottom portion of Fig. 5, while the theoretical band structure is depicted with the dashed curve. The agreement between experiment and theory is improved with respect to our earlier work, and is visibly better for the dashed-dotted curve, which deviates from theory by 0.5 eV at the top and 0.7 eV at the bottom of the band.

In order to confirm that the position of the Δ_1 band determined in our earlier study² had indeed been affected by the presence of Fe, at the end of the present experiments we intentionally annealed sample *A* to about 750°C for 30 min. AES scans showed that surface con-

centration of Fe was about the same as in the earlier work. The EDC's collected from this surface were indeed found to be very similar to those presented in Fig. 2 of Ref. 2, as expected.

IV. CONCLUSION

The electron band structure of Tb has been reexamined by means of angle-resolved photoemission experiments on a Tb(0001) sample with no Fe impurity in the surface region. Comparison with the data collected earlier on an Fe-contaminated sample shows that the presence of Fe in

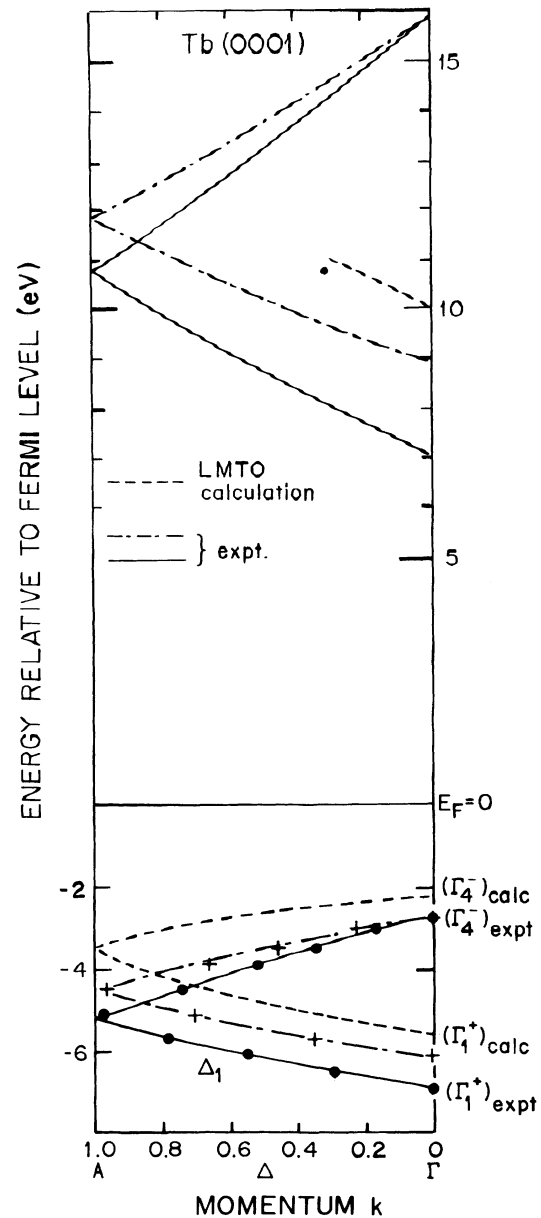


FIG. 5. Electron band structure of Tb along the $\Gamma\Delta A$ line. Dashed curves represent theory. Solid and dashed-dotted curves represent experiment with different choice of the position of the bottom of the band (see text).

the surface region affected the position of the Δ_1 band, especially in the top portion of the band, the effect consisting in a shift of the band toward larger binding energies. This effect can be explained by the repulsion between the Fe 3d and the Tb 5d electrons. The data from the clean surface are in good agreement with theory with regard to dispersion and width of the initial Δ_1 band, although the absolute energy position deviates from theory on average by -0.6 eV.

ACKNOWLEDGMENTS

We acknowledge partial support of this work by the Department of Energy with Grant No. DE-FG02-86ER45239. One of us (S.C.W.) is also indebted to the Science and Technology Commission of the People's Republic of China for partial support by the National Natural Science Foundation through Grant No. 9187002.

*On leave from Department of Physics, Peking University, The People's Republic of China.

†Present address: The BOC Group, Technical Center, Murray Hill, NJ 07974.

¹F. P. Netzer and J. A. D. Matthew, *Rep. Prog. Phys.* **49**, 621 (1986).

²S. C. Wu, H. Li, D. Tian, J. Quinn, Y. S. Li, J. Sokolov, and N. E. Christensen, *Phys. Rev. B* **41**, 11 911 (1990).

³J. Quinn, Y. S. Li, F. Jona, and D. Fort, *Surf. Sci.* **257**, L647 (1991).

⁴S. C. Wu, H. Li, Y. S. Li, D. Tian, J. Quinn, F. Jona, and D. Fort, *Phys. Rev. B* **44**, 13 720 (1991).

⁵Y. Dai, H. Li, and F. Jona, *Rev. Sci. Instrum.* **61**, 1724 (1990).

⁶F. Gerken, A. S. Flodström, J. Barth, L. I. Johansson, and C. Kunz, *Phys. Scr.* **32**, 43 (1985).

⁷J. J. Yeh and I. Lindau, *At. Data Nucl. Data Tables* **32**, 1 (1985).

⁸*Photoemission in Solids I, General Principles*, edited by M. Cardona and L. Ley (Springer, Berlin, 1978).

⁹C. J. Ballhausen and H. B. Gray, *Molecular Orbital Theory* (Benjamin, New York, 1965), p. 38; V. L. Moruzzi, A. R. Williams, and J. F. Janak, *Phys. Rev. B* **10**, 4856 (1974).

¹⁰W. Eberhardt, S. C. Wu, R. Garrett, D. Sondericker, and F. Jona, *Phys. Rev. B* **31**, 8285 (1985).

¹¹Z. Q. Wang, S. C. Wu, J. Quinn, C. K. C. Lok, Y. S. Li, F. Jona, and J. W. Davenport, *Phys. Rev. B* **38**, 7442 (1988).

¹²D. LaGrafte, P. A. Dowben, and M. Onellion, *Phys. Rev. B* **40**, 3348 (1989).

¹³A. J. Freeman, in *Magnetic Properties of Rare-Earth Metals*, edited by R. J. Elliott (Plenum, London, 1972), p. 245.